Liquid Crystals
Publication details, including instructions for authors and subscription information:
http://www.informaworld.com/smpp/title~content=t713926090

Molecular dynamics and X-ray scattering simulations of cyclic siloxane-based liquid crystal mesogens

Edward P. Socci[a]; Barry L. Farmer[a]; Timothy J. Bunning[b]; Ruth Pachter[c]; W. Wade Adams[c]
[a] Department of Materials Science and Engineering, University of Viginia, Charlottesville, Virginia, U.S.A. [b] Department of Chemical Engineering, University of Connecticut, Storrs, Connecticut, U.S.A. [c] Wright Laboratory, Materials Directorate, WL/MLPJ, Wright-Patterson Air Force Base, Ohio, U.S.A.

To cite this Article Socci, Edward P. , Farmer, Barry L. , Bunning, Timothy J. , Pachter, Ruth and Adams, W. Wade(1993) 'Molecular dynamics and X-ray scattering simulations of cyclic siloxane-based liquid crystal mesogens', Liquid Crystals, 13: 6, 811 — 827
To link to this Article: DOI: 10.1080/02678299308027295
URL: http://dx.doi.org/10.1080/02678299308027295

LIQUID CRYSTALS, 1993, VOL. 13, NO. 6, 811–827

Molecular dynamics and X-ray scattering simulations of cyclic siloxane-based liquid crystal mesogens

by EDWARD P. SOCCI and BARRY L. FARMER
Department of Materials Science and Engineering, University of Viginia, Charlottesville, Virginia 22903, U.S.A.

TIMOTHY J. BUNNING
Department of Chemical Engineering, University of Connecticut, Storrs, Connecticut 06268, U.S.A.

RUTH PACHTER* and W. WADE ADAMS
Wright Laboratory, Materials Directorate, WL/MLPJ, Wright-Patterson Air Force Base, Ohio 45433-7702, U.S.A.

(*Received 28 May 1992; accepted 22 December 1992*)

Molecular dynamics simulations of cyclic siloxane-based liquid crystals offer new insights into the conformational flexibility of these materials. Interdigitation between the cholesteryl-4′-allyloxybenzoate and biphenyl-4′-allyloxybenzoate mesogens pendant on the cyclic siloxane ring is observed in the simulated structures. All molecular models considered viz. disc, cone, and cylinder, display a large conformational flexibility, which is important regarding the liquid crystalline phase behavior. The disc molecular model exhibits the largest flexibility as indicated by mean dihedral angles and their range for certain principal torsions, evaluated from the molecular dynamics simulations. Results from the dynamics simulations of cylinder molecular pairs indicate a significant amount of conformational flexibility in the siloxane rings. The degree of interdigitation between mesogens is dependent on the flexibility of the siloxane rings, as shown by calculations for a fixed ring system resulting in less interdigitation, also reflected in calculated X-ray scattering sections along the starting molecular direction. Weaker molecular transforms were observed for the non-fixed system due to a lack of boundary conditions. In general, the qualitative agreement of the starting structure's reflections and those shown by the experimental data is encouraging.

1. Introduction

A variety of side chain liquid crystalline (LC) polysiloxanes have been synthesized and characterized including those exhibiting calamitic and discotic phases (a recent review of the liquid crystalline behavior of linear polysiloxanes is given in [1]). These compounds find uses as stationary phases for high resolution gas chromatography columns [2, 3], read–write optical storage media [4, 5], photochromic and photosensitive media [6, 9], ferroelectric display materials [10, 12], and as non-linear optical materials [13]. Considerable effort has been expanded in examining the molecular packing of these compounds considering their highly flexible backbones. Recent X-ray examinations have indicated a microphase separated morphology induced by a thermodynamic immiscibility between the random coil backbones and the rod-like

* Author for correspondence.

0267–8292/93 $10·00

mesogens [14–17]. When these two groups are chemically dissimilar, microphase separation is enhanced [18]. Electron density calculations indicate a partitioned molecular system consisting of sublayers of mesogens, spacer groups, and backbones [17]. Of increasing recent interest are liquid crystalline systems consisting of siloxane rings with a variety of pendant mesogen groups attached. Several studies have been reported on the optical and thermal behaviour of these compounds [19–21]. One such system, consisting of cyclic(pentamethylsiloxane) with combinations of cholesteryl-4′-allyloxybenzoate {C} and biphenyl-4′-allyloxybenzoate {B} mesogens LC{BC} shown in figure 1 (*a*) was studied in detail [22, 23], and examined for attributes to light processing media [24–26].

In general, unlike linear systems, a small siloxane ring having mesogenic units attached by short spacer chains might have intramolecular constraints that preclude certain kinds of inter-mesogen interactions. Monte Carlo simulations [27, 28] have predicted phases ranging from discotic to the conventional nematic, depending on the size of the ring and the rigidity and length of the leader group used to attach the mesogenic groups. Recent experimental data suggests that these compounds form calamitic phases and exhibit well-defined interlayer order [20, 23]. However, systematic studies of the molecular packing characteristics for cyclic siloxane-based compounds have not been reported.

As part of an ongoing effort to complement the understanding of the structure–property relationships found in siloxane liquid crystals, we have carried out a series of molecular simulations. Molecular mechanics simulations based on models of LC {BC} containing 40 mol% {C} and 60 mol% {B} [29] and highly interdigitated LC {B} [30] have been performed. The preference towards interdigitation of the {B} mesogens was clearly shown also by an application of the force feedback ARM [31]. The calculated meridional scattering sections lent qualitative support to one of the previously proposed structural models for an interpretation of the X-ray diffraction data (cf. figure

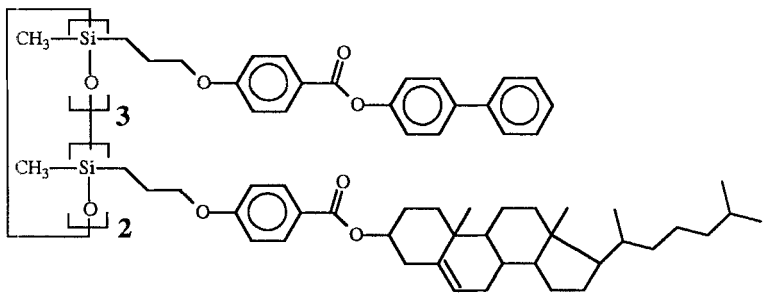

(*a*)

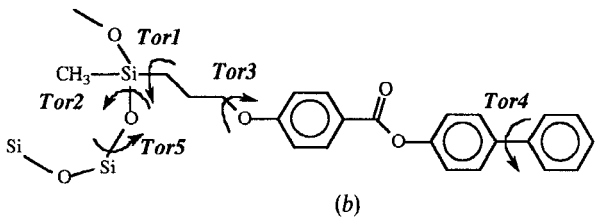

(*b*)

Figure 1. The chemical structure of the studied cyclic siloxane-based liquid crystal (*a*) and the torsions examined within the structure (*b*).

7 in [23] for structural details). We report here molecular dynamics calculations where an insight into the conformational flexibility and molecular arrangements and organization of LC{BC} is obtained. The investigation provides an assessment of their relative stability, and the results indicate the degree of conformational flexibility among the pendant mesogens of the LC{BC} molecular system, and its effects on mesogen interdigitation. In addition to the structure–property relationships which may be derived from this study, the calculations are of importance in understanding the role of the siloxane core as flexible backbone for the attachment of optically non-linear chromophores [32]. Indeed, molecular dynamics simulations proved useful in studying chromophore-bound polypeptides [33].

2. Computational methods

Molecular mechanics is a well-established approach for macromolecular structural definition [34] at the atomic level, applied, for example, to polymeric chains [35 a, b], and also to liquid crystalline systems [36], while in this study the CHARMm [37] functional form for the force field was used. Although this molecular mechanics potential was initially developed for biomolecules, the present version [38 (a)] includes an updated force field parameter set for general organic molecules and hetero-atoms [38 (b)], particularly for organosiloxane derivatives. These potentials were successfully applied in the conformational study of octamethylcyclotetrasiloxane [39], and the force constants are therefore considered appropriate for the application to the comparable ten-membered cyclic siloxane-based structures. However, the standard partial atomic charges for the electrostatic contribution to the non-bonded potential energy for the Si and O atoms were not appropriate and needed to be modified [40]. Indeed, one of the shortcomings in structure determination by the molecular mechanics methodology is found in the use of standard partial atomic charges for this contribution to the force field. The use of an improved electron distribution within a particular force field has proved important, especially for cyclic molecular systems [41, 42].

This modified potential energy for the molecular system is utilized for the molecular dynamics (MD) simulation [43] at elevated temperatures for calculating structural fluctuations, phase transitions and time averaged properties, used to partition the total energy between kinetic and potential contributions, and to distribute the latter among the vibrational states of the molecule. In general, a molecular dynamics simulation consists of heating, equilibration and simulation periods [43]. Specifically, heating to 300 K is accomplished by slowly and uniformly adding kinetic energy to the molecular system at periodic time intervals by assigning velocities to each atom, either randomly or in proportion to the force acting on the atom. The length of the heating period depends on the size of the molecular system ($\approx$2 ps in this case). An equilibration is then carried out at 300 K until no systematic changes in temperature are evident, and the total energy is conserved. The dynamics simulation is carried out after full equilibration has been achieved by continuing to integrate the equation of motion, so that time averaged results and other statistical or thermodynamic information can be obtained. This protocol was followed with the energy and temperature examined after each stage to ensure trajectory accuracy.

The modelling of scattering from an oriented material with cylindrical symmetry, without assuming any crystalline order, is ordinarily achieved by applying the cylindrically averaged scattering technique [44]. The averaging is accomplished by a rotation around the axis of the direction of the fibrous microscopic model (by

convention the z axis), so that the intensity transform is cylindrically symmetrical about it. This simulation is applicable for highly oriented materials, such as fibres and in this case liquid crystals [44]. Spurious features which may occur in this diffraction simulation of molecular models are eliminated by using a model size correction, in which the cylindrically averaged scattering is subtracted from that derived for a prism, or cylinder, with the same radial structure as the model but structureless in the z direction. Such a calculation describes a special case of the general formulation [44]. This total scattering, including the model size correction as well as the Fourier transform of the projection of the structure onto the z axis (meridional section) were calculated by the CERIUS simulation program [45].

3. Results and discussion

3.1. *Molecular dynamics*

3.1.1. *Isolated models*

Six isomers of the cyclic penta(methylsiloxane) molecular system describing the relative position of the methyl groups to the ring: specifically, relative orientations of {five axial:zero equatorial}to{zero axial:five equatorial}, respectively, of the symmetry canonical form, were initially considered and studied in detail [29]. The criterion used to select the three starting conformations of the basic ring system for the determination of global molecular topology of LC{BC} is based on the experimental data. In particular, the extreme conformations in which the mesogens are either equatorial or axial, respectively, and an intermediate conformation having two cholesteryl-4′-allyloxybenzoate {C} side chains at an axial position and three biphenyl-4′-allyloxybenzoate {B} mesogens at an equatorial position. The fragments were constructed by using standard geometry parameters, and then merged with the siloxane ring one mesogen at a time, rotating for best conformation (by distance) around the siloxane ring-{BC} rotatable bond. The geometry was then optimized using first the steepest descent method, followed by the conjugate gradient technique for the complete potential energy minimization. The geometry optimization was performed with no constraints, so that the cyclic structure was allowed to respond to changes in the relative position of the methyl groups and mesogenic side chains. This approach minimizes the possibility of calculating a local minimum in the energy potential. However, it should be stressed that no systematic conformational space search was performed at this level of modelling and only those global molecular topologies consistent with the experimental data are studied at this stage.

Details of the molecular dynamics simulations carried out for these molecules are listed in table 1 (*a*). A comparison of the structural features of the starting models and those determined from the MD calculation of 10 ps at 300 K indicate a large amount of conformational variation (see, for example, the starting and lowest energy structures of the MD run for the disc isomer in figures 2 (*a*) and (*b*). A detailed analysis was carried out by comparing various torsional angles during the simulation to those in the initial structure. The five torsions examined are shown in figure 1 (*b*). The mean variation of a torsion angle during the MD run is derived from a histogram plot of the dihedral angle distribution during the simulation, from which the mode can be determined. This, in turn, approximates the mean since a normal distribution is generally observed. The distribution of torsional angles is described in the following by the range. In all cases, the initial model was related to an equilibrated dynamics structure, and deviations from this equilibrated structure during the MD run were assessed.

Table 1. Details of molecular dynamics simulation†.

	Cone‡	Disc‡	Cylinder§
(*a*) Isolated cone, disc and cylinder models.			
Heating time ps	0·5	0·5	2·5
Equilibrium time ps	64·0	5·5	41·5
Simulation time ps	10·0	10·0	10·0
Time step ps	0·0005	0·0005	0·001
(*b*) Unconstrained cylinder molecular pair (CASE I)§.			
Heating time ps		2·5	
Equilibrium time ps		130·0	
Simulation time ps		10·0	
Time step ps		0·0005	
(*c*) Constrained cylinder molecular pair (CASE II)§.			
Heating time ps		5·0	
Equilibrium time ps		40·0	
Simulation time ps		10·0	
Time step ps		0·001	
(*d*) Constrained disc molecular pair (CASE III)§.			
Heating time ps		5·0	
Equilibrium time ps		10·0	
Simulation time ps		10·0	
Time step ps		0·0001	

† Non-bonded cut off distance: 8 Å; non-bonded pair list update frequency: every 50 iterations.

‡ SHAKE procedure not applied.

§ SHAKE procedure applied.

Table 2 (*a*) summarizes the mean and range ($\approx$ the standard deviation*4 for the case of a normal distribution) of the Tor1 $\{O\text{–}Si\text{–}C_{\text{first of spacer mesogen}} - C_{\text{second of spacer mesogen}}\}$ dihedral angles from the dynamics simulation. Notably, the largest conformation flexibility around this bond is observed in the cone model, with two of the dihedral angles (on {B} mesogens) varying by an average of 104°, and 147° from the initial magnitudes, while all other $\langle$Tor1$\rangle$ differences are smaller than 30°. Large variations of this dihedral angle may reflect, in part, the relative instability of a particular model with respect to the proximity of the mesogens. Thus, the result is anticipated since the cone model is the least stable energetically (the minimum energies of the initial cone disc, and cylinder models are 309, 298, and 260 kcal mol^{-1}, respectively) [29]. Also, the average $\langle\Delta$Tor1$\rangle$ values are 61°, 13°, and 7° for the cone, disc, and cylinder models, respectively. This relative flexibility of the cone model is also reflected in the range of values shown in table 2 (*a*) (average = 49°), which are much smaller than those for the disc model (= 94°). This may be due to an increase in the steric interactions among the mesogens for the cone relative to the disc model. Interestingly, the mesogens of the cylinder model

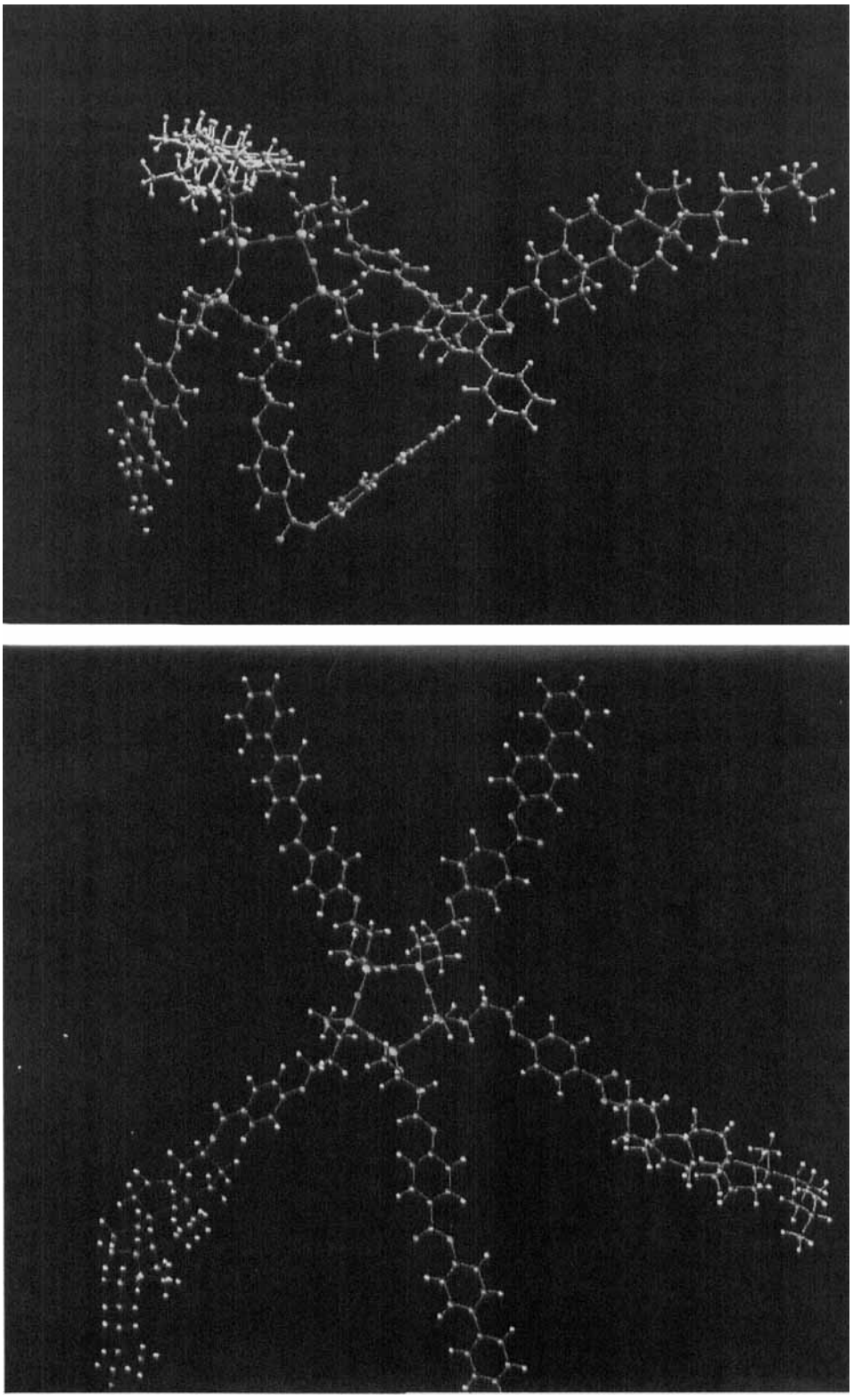

(*a*) (*b*)

Figure 2. Model structures of the disc isomer (*a*) the starting structure; (*b*) the lowest energy conformation adopted during the MD simulation.

Table 2. Mean and Δ† dihedral angles and range (in brackets) from the MD simulation in comparison to the initial values.

Mesogen type (*a*)‡		Isolated cone		Isolated disc		Isolated cylinder	
		⟨Tor1⟩	⟨ΔTor1⟩	⟨Tor1⟩	⟨ΔTor1⟩	⟨Tor1⟩	⟨ΔTor1⟩
{C}	Initial	60°		63°		185°	
	MD	55° (49°)	5°	74° (88°)	11°	176° (56°)	9°
{C}	Initial	45°		59°		300°	
	MD	68° (50°)	23°	54° (62°)	5°	283° (38°)	17°
{B}	Initial	180°		54°		60°	
	MD	153° (50°)	27°	65° (170°)	11°	66° (84°)	6°
{B}	Initial	180°		175°		61°	
	MD	284° (56°)	104°	195° (76°)	20°	64° (58°)	3°
{B}	Initial	40°		55°		69°	
	MD	187° (42°)	147°	71° (74°)	16°	67° (41°)	2°
(*b*)		⟨Tor2⟩	⟨ΔTor2⟩	⟨Tor2⟩	⟨ΔTor2⟩	⟨Tor2⟩	⟨ΔTor2⟩
{C}	Initial	304°		176°		184°	
	MD	184° (69°)	120°	295° (86°)	119°	189° (36°)	5°
{C}	Initial	306°		176°		309°	
	MD	172° (62°)	134°	49° (90°)	127°	59° (68°)	110°§
{B}	Initial	303°		194°		298°	
	MD	63° (60°)	120°§	183° (78°)	11°	169° (117°)	129°
{B}	Initial	305°		176°		293°	
	MD	59° (66°)	114°§	176° (169°)	0°	282° (67°)	11°
{B}	Initial	299°		54°		175°	
	MD	181° (49°)	118°	293° (90°)	121°§	77° (96°)	98°
(*c*)¶		⟨Tor3⟩	⟨ΔTor3⟩	⟨Tor3⟩	⟨ΔTor3⟩	⟨Tor3⟩	⟨ΔTor3⟩
{C}	Initial	177°		177°		179°	
	MD	173° (55°)	4°	184° (179°)	7°	188° (48°)	9°
{C}	Initial	185°		170°		179°	
	MD	148° (103°)	37°	185° (137°)	15°	177° (43°)	2°
{B}	Initial	119°		183°		76°	
	MD	190° (58°)	71°	294° (137°)	111°	179° (72°)	103°
{B}	Initial	171°		173°		85°	
	MD	202° (52°)	31°	161° (94°)	12	169° (41°)	84°
{B}	Initial	91°		175°		183°	
	MD	186° (52°)	95°	165° (78°)	10°	171° (71°)	12°
(*d*)‖		⟨Tor4⟩	⟨ΔTor4⟩	⟨Tor4⟩	⟨ΔTor4⟩	⟨Tor4⟩	⟨ΔTor4⟩
{B}	Initial	0°		0°		−2°	
	MD	9° (46°)	9°	6° (43°)	6°	6° (35°)	8°
{B}	Initial	0°		0°		10°	
	MD	−6° (78°)	6°	−12° (88°)	12°	−2° (72°)	12°
{B}	Initial	0°		0°		−6°	
	MD	−4° (87°)	4°	−9° (1°)	9°	−12° (73°)	6°

† The mean variation of the torsion as compared to the initial value.
‡ Tor1 = {O–Si–$C_{\text{first of spacer mesogen}}$ – $C_{\text{second of spacer mesogen}}$}.
§ Tor2 = {Si–O–Si–$C_{\text{first of spacer mesogen}}$}.
¶ Tor3 = {C–C–O–{phenyl}}.
‖ Rotatable bond between the two phenyl rings in the three {B} mesogens.

exhibit a lower conformational flexibility than those in the disc, also confirmed by a lower average range of torsion angles (=55°).

Tor2 {Si–O–Si–$C_{\text{first of spacer mesogen}}$} torsions were also examined. The results tabulated in table 2(*b*) indicate that the largest conformational flexibility around this bond is observed for the cone model, where all of the dihedral angle differences are in the range of ±120°. Specifically, two of the mesogens which had an initial Tor2 torsion of −60° with respect to the siloxane ring assume mean values of *c.* 180°, thus resembling the cylinder model. The average ⟨ΔTor2⟩ values are 121°, 75°, and 71° for the cone, disc, and cylinder models, respectively. In general, all three models exhibit large changes in the mesogen's orientation relative to the siloxane ring. The range of torsion angles was calculated to be approximately 60° for both the cone and cylinder models, while a larger range is observed for the disc model, as can be clearly seen in figure 2(*b*). The greatest possibility for conformational flexibility in the position of the mesogens relative to the siloxane ring is exhibited by the disc model. This can be explained, in part, by lower steric interactions between mesogens in this case, enabling easier reorientation.

The ability of the mesogens to rotate with respect to the leader group is described by the torsion Tor3 (C–C–O–{phenyl}). In order to be consistent with the proposed model of interdigitation [23, 29], the mesogens would in some instances need to be splayed (kinked) with respect to the director in order to maintain continuous lamellar packing. A primary location for this kinking to take place may be at this ester bond. The results summarized in table 2(*c*) indicate that the disc model has the greatest range (=64°, 125°, and 55° for the cone, disc, and cylinder models, respectively) and the lowest average difference in the mean dihedral angles (=48°, 31°, and 42° for the cone, disc, and cylinder models, respectively). The average range for the disc model is almost twice that of the cone and cylinder models, which may foretell a greater tendency towards interdigitation for this model. It is interesting to point out that with the exception of the disc model (which has one *gauche* bond), all of the mean ⟨Tor3⟩ values derived from the dynamics simulation assume a nearly *trans* orientation of approximately 180°. Small differences between the rotatable bonds of the two phenyl rings in the {B}mesogens (Tor4) were observed (see table 2(*d*)). Evidently, the effects of neighbouring mesogens cause this torsion to deviate from the experimental value of biphenyl of approximately 44° in the gas phase [46], and *c* 34°–37° in a nematic liquid crystalline state [47]. The final set of dihedral angles examined were those within the siloxane ring (Tor5 = {Si–O–Si–O(1) and O–Si–O–Si(2)} (see table 3). The results indicate the large amount of flexibility and conformational variation present in the siloxane ring. Once again, the disc model exhibits the greatest flexibility, supporting the assumption that the disc may be the most favourable conformation in a liquid crystalline phase.

Changes in the Tor1, Tor2, Tor3 and Tor5 torsional angles indicate that the disc model exhibits a larger conformational flexibility than the cylinder and cone models. Especially indicative are the large range, yet the relatively small difference between the initial and mean MD dihedral angles for the disc model. The advantage in flexibility for the disc may be important with regard to the liquid crystalline phase behaviour observed for these materials. In general, the amount of interdigitation is primarily governed by the flexibility of the leader groups and intermolecular interactions of nearby mesogens [48]. Also important is the persistence of the interdigitation, which may also be influenced by the conformational flexibility. Based on these two criteria, the results may support the disc molecular model as the basis for an arrangement of a highly interdigitated, splayed mesogenic liquid crystalline phase. Note that although

the disc, cone, and cylinder structures have changed considerably during the molecular dynamics simulation, they are still termed as such in order to be able to distinguish the different starting models.

3.1.2. *Molecular pairs*

Molecular dynamics simulations were carried out on molecular pairs, where the intermolecular ordering patterns considered for the global molecular topologies were based on the 'interdigitation of mesogens' supposition established from the experimental data [23]. In particular, the cylinder and disc models were analysed at this stage, since the cone model was shown to be less stable, and resume a cylinder type geometry during the simulation. Previous X-ray diffraction measurements made on these cyclic siloxane-based liquid crystals manifest a primary *d*-spacing of ~ 25 Å [23], corresponding to the partial interdigitation of the {B} and {C} mesogens in a classic S_{Ad}-like structure [48]. Molecular dynamics simulations may indicate to what degree the {B} and {C} mesogens remain interdigitated.

The starting molecular arrangement for the MD run (details of which are presented in table 1 (*b*)) is described in detail elsewhere [29]. Since no constraints are applied to the siloxane rings in these molecules (CASE I), they do not remain parallel to one another as shown in figures 3 (*a*) and (*b*). This freedom of rotation may not be as energetically favourable in the liquid crystalline phase due to constraints from other nearby molecules in the system, partially dealt with by constraining the siloxane rings (CASE II). Specifically, in order to eliminate the ability of the siloxane rings to change their relative orientation, an additional calculation was carried out, in which atom constraints were applied to all the siloxane rings atoms. By constraining the rings it is expected that the effects of the liquid crystalline phase would be better modelled. The details of the molecular dynamics calculation are given in table 1 (*c*).

It is interesting to note a degree of interdigitation amongst the {B} and {C} mesogens after the dynamics simulation in CASE I, comparable to that seen in the minimum energy starting structure. This supports the proposed S_{Ad}-like packing structure [23] with extensive interdigitation of the pendant groups. During the simulation of 140 ps (including equilibration), no tendency of the system to separate was observed. The conformational flexibility of the interior mesogens as shown by changes in the torsion angles, was also examined. In general, Tor1 varies in a range of 30° to 60° for the interior mesogens of this cylinder pair model, as shown in table 4 (*a*). An examination of the variation in one of the Tor1 angles during the simulation shows that there is no remarkable difference in the conformational flexibility or stability of the interdigitated mesogens when compared to the results for an isolated cylinder. In both cases, the differences in the dihedral angles are small and the range similar, except for one of the torsions which changes from an initial value of 69° to a mean value of 181° during the simulation. The average range for the interdigitated mesogens is slightly lower due to possible interactions introduced upon packing. Similarly, the statistical data for Tor3 shown in table 4 (*b*) reveals little difference between the results for the interdigitated molecular pair structure and the isolated cylinder, and only two of the angles change markedly during the simulation. In both cases, there is a tendency of these orientations to assume values of *ca.* 180°. It is interesting to point out that a relatively small range of changes in Tor2 are observed in both molecules in the pair, showing only a small change in the amount of interdigitation, while larger deviations are noted for Tor4. On the other hand, larger changes are observed in Tor5 for the cylinder pair than for the isolated cylinder model, with the average magnitudes of

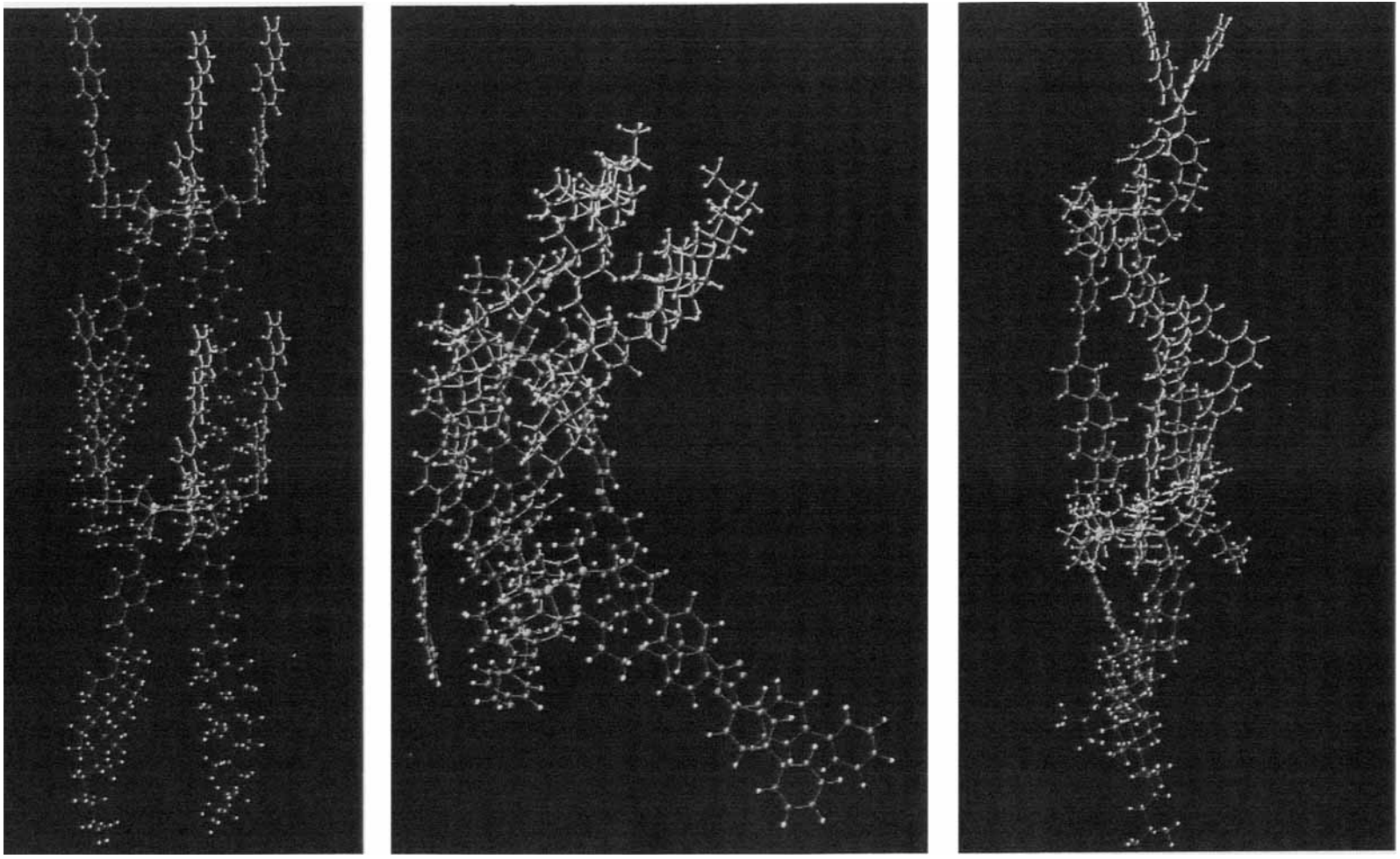

(*a*) (*b*) (*c*)

Table 3. ⟨Tor5⟩† and ⟨ΔTor5⟩‡ mean dihedral angles and range (in brackets) from the MD simulation in comparison to the initial values.

		Isolated cone		Isolated disc		Isolated cylinder	
Type		⟨Tor5⟩	⟨ΔTor5⟩	⟨Tor5⟩	⟨ΔTor5⟩	⟨Tor5⟩	⟨ΔTor5⟩
1	Initial	60°		290°		187°	
	MD	182° (53°)	122°	292° (69°)	2°	287° (84°)	100°
2	Initial	59°		76°		177°	
	MD	183° (56°)	124°	54° (79°)	22°	52° (11°)	125°
1	Initial	299°		299°		285°	
	MD	66° (58°)	127°§	64° (68°)	125°§	181° (73°)	104°
2	Initial	299°		59°		64°	
	MD	292° (62°)	7°	297° (4°)	122°§	175° (64°)	111°
1	Initial	300°		293°		58°	
	MD	70° (63°)	130°§	182° (113°)	111°	57° (43°)	1°
2	Initial	60°		66°		297°	
	MD	304° (64°)	116°§	184° (78°)	118°	310° (39°)	13°
1	Initial	297°		297°		208°	
	MD	173° (69°)	124°	315° (60°)	18°	178° (76°)	30°
2	Initial	64°		59°		173°	
	MD	176° (65°)	112°	61° (59°)	2°	170° (72°)	3°
1	Initial	300°		68°		298°	
	MD	64° (49°)	124°§	179° (77°)	111°	276° (91°)	22°
2	Initial	161°		295°		56°	
	MD	302° (47°)	41°	173° (87°)	122°	143° (94°)	87°

† Siloxane ring torsions: {Si–O–Si–O$^{\text{Type 1}}$ and O–Si–O–Si$^{\text{Type 2}}$}.
‡ The mean variation of the torsion as compared to the initial value.
§ The absolute value of the variation is given.

Table 4. Mean, Δ dihedral angles and range from the MD simulation in comparison to the initial values for the unconstrained cylinder pair model.

					Isolated cylinder	
(*a*)	Initial Tor1	⟨Tor1⟩	⟨ΔTor1⟩	Range	⟨ΔTor1⟩	Range
{C}	185°	177°	8°	39°	9°	41°
{C}	300°	292°	8°	36°	17°	56°
{B}	69°	181°	112°	40°	6°	38°
{B}	61°	55°	6°	46°	3°	84°
{B}	60°	56°	4°	59°	2°	58°
(*b*)	Initial Tor3	⟨Tor3⟩	⟨ΔTor3⟩	Range	⟨ΔTor3⟩	Range
{C}	179°	193°	14°	344°	116°	41°
{C}	179°	181°	2°	43°	12°	71°
{B}	76°	197°	112°	70°	103°	72°
{B}	85°	187°	4°	55°	9°	48°
{B}	183°	258°	182°	36°	2°	43°

$\langle \Delta Tor5 \rangle$ being larger by 35° and 18°. The average range is larger by 27° for the siloxane ring than that for the isolated cylinder case. This indicates that the siloxane ring undergoes a large amount of torsional change during the simulation when the mesogens are interdigitated. Indeed, the ten-membered siloxane ring itself is very flexible, as has been shown by molecular dynamics calculations we initially performed. For example, the all-atom RMSD differences between the initial minimized structure, and the last and average structures of the molecular dynamics simulation were calculated to be 1·6 Å and 1·4 Å, respectively.

The results of the MD calculation in CASE II show less interdigitation than in CASE I, as the pendant mesogens, especially {B}, move outward from the central region between the siloxane rings. An examination of the changes in the torsions during the dynamics calculation reveal differences between CASE I and CASE II of the molecular pairs simulations. Table 5 lists the data from the interior mesogens for the constrained cylinder molecular pair model. The average range of flexibility for this model of *c.* 90° is much larger than those for the isolated or unconstrained cylinder models. The results for this model also demonstrate a larger average difference between initial and mean dihedral angles (=61°). By constraining the siloxane ring, larger torsional movements of the leader group near the siloxane ring (Tor1) are observed, while the range and average differences for the Tor3 torsions are similar to those of the unconstrained case because it is several atoms away. Contrary to this behaviour, the Tor2 values, and also those of Tor4 and Tor5, do not change as much as in the unconstrained case resulting from the hindrance to ring movement.

The partial interdigitation of the mesogens in the disc model may also correspond to the observed X-ray data. Molecular dynamics calculations (details are given in table 1 (*d*)) were thus performed on two interdigitated disc molecules, each minimized to its minimum energy conformation. Atom constraints were imposed on the rings in order to maintain their relative initial orientation. Statistical data for the Tor1 torsions show relatively large variations analogous to the constrained cylinder molecular pair model. Indeed, it is interesting to note that the so-called disc model transforms into a conformation more resembling the cone model.

3.2. *X-ray diffraction simulations*

Simulated X-ray diffraction patterns of the molecular pair systems (CASES I and II) were examined. The simulated meridional scattering patterns (along the long axis of the cylinder from the starting cylinder molecular pair model (START), and the lowest energy structure from the MD runs of the unconstrained and constrained cases are

Table 5. Mean dihedral angles and range for the $\langle Tor1 \rangle$ torsion for the constrained molecular pair of cylinder models.

Mesogen type	Initial	Mean dynamics	Difference	Range	Isolated cylinder Difference	Isolated cylinder Range
{C}	185°	82°	103°	129°	9°	41°
{C}	300°	300°	0°	39°	17°	56°
{B}	69°	79°	10°	38°	6°	38°
{B}	61°	115°	54°	187°	3°	84°
{B}	60°	200°	140°	44°	2°	58°

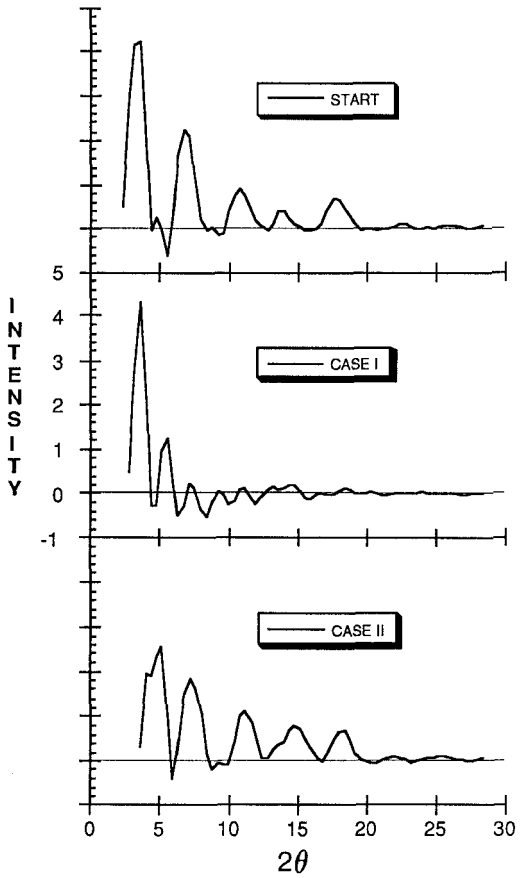

Figure 4. Simulated meridional scattering sections for the unconstrained (CASE I), constrained (CASE II), and starting (START) structures. Y scales are the same on all three curves and have been reduced by 10^6.

Table 6. X-ray diffraction maxima (Å) from calculated meridional scattering patterns of the experimental, starting, and lowest energy of the unconstrained and constrained MD structures.

Experimental	START	CASE I	CASE II
49·0			
24·4	24·8	24·8	17·1
12·0	13·1	15·9	12·4
8·0	8·3	12·4	8·0
6·2	6·4		6·0
	5·1		4·8

shown in figure 4. Table 6 lists the *d*-spacings of the reflections for all cases. Small 2θ values were omitted due to a large peak induced by the relatively small number of units [29]. A low angle reflection observed experimentally due to cholesterol–cholesterol interactions [23] does not appear in the calculated patterns. The experimental 24 Å reflection is due to a layered packing scheme consisting of interdigitated cholesterol and biphenyl mesogens [23]. The remaining periodic reflections have been attributed to short range order observed in some side chain liquid crystalline polymers [49].

Table 6 indicates that the reflections from the START system are similar to those observed experimentally. The molecular transform of the unconstrained system (CASE I) shows much weaker reflections compared to the START system due to a decrease in the uniaxial behaviour of the mesogens along the *z* axis. Correlation is weakened due to the mesogens tendency not to stay parallel to one another along the *z* axis. The constrained system (CASE II) shows reflections similar to the starting structure except that the 24 Å reflection has become slightly smaller. Note, however, that although several of the mesogens rotated out of the interdigitated core, the bulk of the structure remained parallel to the *z* axis. It should be stressed that since the liquid crystalline state boundary conditions are not fully taken into account in this study, the result reveals the highly ordered state of this LC. Moreover, these calculations indicate the importance of intra- and intermolecular interactions among the mesogens during the molecular dynamics simulation.

4. Concluding remarks

Molecular dynamics simulations offer new insights into the conformational flexibility of cyclic siloxane-based liquid crystals. Interdigitation between the {C} and {B} mesogens pendant on the siloxane ring is certainly present in the simulated structure, but a quantitative measure of the interdigitation is still to be caclulated, by the application of boundary conditions. The isolated disc model exhibited the most flexibility and greatest stability as indicated by mean dihedral angles and their distribution for certain principal torsions. All three isolated models displayed large conformational flexibility, which will be more constrained in the liquid crystalline phase. Results from the dynamics simulation of the cylinder molecular pairs indicate the conformational flexibility of the siloxane rings, with the changes of the interdigitated mesogens higher for a fixed ring system. X-ray scattering pattern calculations for the lowest energy structures generated during the dynamics run reflect these changes. The qualitative agreement of the starting structure's reflections and those shown by the experimental data is encouraging.

In general, it should be pointed out that the importance of such a simulation is in obtaining an understanding of the molecular arrangement and organization within this LC, in order to lend support to the structural suppositions based on the experimental X-ray data. Indeed, this investigation outlines an initial scheme for the computationally demanding problem of molecular modelling of such large and complex molecular systems, serving as the basis for further studies of liquid crystalline models, for example, the comparison of various siloxane-based macromolecules, mesogen modelling, and the calculation of internal structural changes to be used for statistical average for the diffraction pattern prediction. This molecular simulation offers an initial step towards the derivation of a general modelling strategy to be used in future molecular design studies of materials that exhibit well-defined interlayer order.

We gratefully acknowledge very useful referee comments.

References

[1] GRAY, G. W., 1989, *Side Chain Liquid Crystal Polymer*, edited by C. B. McArdle (Blackie).

[2] JANINI, G. M., LAUB, R. J., PURNELL, J. H., and TYAGI, G. S., 1989, *Side Chain Liquid Crystal Polymers*, edited by C. B. McArdle (Blackie).

[3] APFEL, M. A., FINKELAMANN, H., JANINI, G. M., LAUB, R. J., LUHMANN, B. H., PRICE, A., ROBERTS, W. L., SHAW, T. J., and SMITH, C. A., 1985, *Analyt. Chem.*, **57**, 651.

[4] COLES, H., and SIMON, R., 1985, *Polymer*, **26**, 1801.

[5] EICH, M., WENDORFF, J. H., RECK, B., and RINGSDORF, H., 1987, *Makromolek. Chem. rap. Commun.*, **8**, 59.

[6] CABRERA, I., KRONGAUZ, V., and RINGSDORF, H., 1987, *Angew. Chem. Int. Ed. Engl.*, **26**, 1178.

[7] KELLER, P., 1990, *Chem. Mater.*, **2**, 3.

[8] CABRERA, I., KRONGAUZ, V., and RINGSDORF, H., 1988, *Molec. Crystals liq. Crystals*, **155**, 221.

[9] CREED, D., GRIFFIN, A., GROSS, J., HOYLE, C., and VENKARARAM, K., 1988, *Molec. Crystals liq. Crystals*, **3**, 34.

[10] HAHN, B., and PERCEC, P., 1987, *Macromolecules*, **20**, 2961.

[11] DUMON, M., NGUYEN, M. T., MAUZAC, M., DESTRADE, C., ACHARD, M. F., and GASPAROUX, H., 1990, *Macromolecules*, **23**, 355.

[12] LEBARNY, P., and DUBOIS, J. C., 1989, *Side Chain Liquid Crystal Polymers*, edited by C. B. McArdle (Blackie).

[13] CARR, N., GOODWIN, M., MCROBERTS, A., GRAY, G., MARSDEN, R., and SCROWSTON, R., 1987, *Makromolek. Chem. rap. Commun.*, **8**, 487.

[14] DIELE, S., OELSNER, S., KUSHEL, F., HISGEN, B., and RINGSDORF, H., 1988, *Molec. Crystals liq. Crystals*, **155**, 399.

[15] DIELE, S., OELSNER, S., KUSHEL, F., HISGEN, B., RINGSDORF, H., and ZENTEL, R., 1987, *Makromolek. Chem.*, **188**, 1993.

[16] PERCEC, V., HAHN, B., EBERT, M., and WENDORFF, J. H., 1990, *Macromolecules*, **23**, 2095.

[17] DAVIDSON, P., LEVELUT, A. M., ACHARD, M. F., and HARDOUIN, F., 1989, *Liq. Crystals*, **14**, 561.

[18] PERCEC, V., and HAHN, B., 1989, *Macromolecules*, **22**, 1588.

[19] RICHARDS, R. D. C., HAWTHORNE, W. D., HILL, J. S., WHITE, M. S., LACEY, D., SEMLYEN, J. A., GRAY, G. W., and KENDRICK, T. C., 1990, *J. chem. Soc. chem. Commun.*, p. 95.

[20] KREUZER, F. H., ANDREJEWSKI, D., HAAS, W., HABERLE, N., RIEPL, G., and SPES, P., 1991, *Molec. Crystals liq. Crystals*, **199**, 345.

[21] BUNNING, T. J., 1991, Technical Report WL-TR-91-4012.

[22] Provided by F. H. KREUZER of the Consortium für Electrochemische Industrie of Germany.

[23] BUNNING, T. J., KLEI, H. E., SAMULSKI, E. T., CRANE, R. L., and LINVILLE, R. J., 1991, *Liq. Crystals*, **10**, 445.

[24] PINSL, J., BRAUCHLE, CHR., and KREUZER, F. H., 1987, *J. molec. Electron.*, **3**, 9.

[25] ORTLER, R., BRAUCHLE, C., MILLER, A., and RIEPL, G., 1989, *Makromolek. Chem. rap. Commun.*, **10**, 189.

[26] TSAI, M. L., CHEN, S. H., and JACOBS, S. D., 1989, *Appl. Phys. Lett.*, **54**, 2395.

[27] EVERITT, D. R. R., CARE, C. M., and WOOD, R. M., 1987, *Molec. Crystals liq. Crystals*, **135**, 55.

[28] EVERITT, D. R. R., CARE, C. M., and WOOD, R. M., 1991, *Molec. Crystals liq. Crystals*, **201**, 41.

[29] PACHTER, R., BUNNING, T. J., and ADAMS, W. W., 1991, *J. Comput. Polymer. Sci.*, **1**, 179.

[30] PACHTER, R., SOCCI, E. P., FARMER, B. L. R., BUNNING, T. J., CRANE, R. L., and ADAMS, W. W., 1992, *Die Makromolekulare Chemie, Theory and Simulations*, in press.

[31] This calculation was carried out in the Molecular Graphics Lab at the Department of Computer Science in the University of North Carolina-Chapel Hill. A collaboration with Dr William Wright in the Department using the force feedback ARM was set up in April 1991. The force feedback ARM uses a parallel MasPar computer (MP-1) operating with 4096 processors in order to calculate the intermolecular energy (using a combination of electrostatic and Lennard–Jones potentials, the parameters used were those of the CHARMm force field) between a rigid structure and a movable docking model. The

resulting force information is used interactively to feed the ARM, so that the best position for the docked structure can be found by manipulating the movable structure on the screen. The structural model can be further improved by an energy minimization. The following experiments were performed:

	Rigid structure	Moveable structure†
1	2{C}†	2{C}†
2	2{C}	3{B}
3	3{B}	2{C}
4	3{B}	3{B}
5	2{C}+2{C} (translation in *y* direction 17 Å)	3{B}
6	2{C}+2{C} (translation in *y* direction 12 Å)	3{B}
7	2{C}+2{C} (translation in *y* direction 12 Å)	2{C}
8	3{B}+3{B} (translation in *y* direction 12 Å)	3{B}
9	3{B}+3{B} (translation in *y* direction 12 Å)	2{C}
10	3{B}+3{B} (translation in *y* direction 12 Å)	3{B}+3{B}
11	2{C}+2{C} (translation in *y* direction 12 Å)	3{B}+3{B}

† 2{C} = two cholesteryl-4′-allyloxybenzoate side chains at an axial position; 3{B} = three biphenyl-4′-allyloxybenzoate mesogens at an equatorial position.

In each case a few starting positions were attempted. The results of these experiments indicate that the interdigitation of the {B} mesogens is qualitatively more favourable in all cases. On the other hand, attempts to dock the {C} system were not successful.

[32] NATARAJAN, L., BUNNING, T. J., CRANE, R. L., and ADAMS, W. W., 1991, *Macromolecules*, **24**, 6554.

[33] PACHTER, R., COOPER, T. M., NATARAJAN, L. V., OBERMEIER, K., CRANE, R. L., and ADAMS, W. W., 1992, *Biopolymers*, **32**, 1129.

[34] ROE, R. J., 1991, *Computer Simulation of Polymers* (Prentice-Hall).

[35] (a) SORENSEN, R. A., LIAU, W. B., and BOYD, R. H., 1988, *Macromolecules*, **21**, 194. (b) RUTLEDGE, G. C., and SUTER, U. W., 1991, *Macromolecules*, **24**, 1921.

[36] DUNMUR, D. A., and WILSON, M. R., 1989, *Molec. Simul.*, **4**, 37.

[37] BROOKS, B. R., BRUCCOLERI, R. E., OLAFSON, B. D., STATES, D. J., SWAMINATHAN, S., and KARPLUS, M., 1983, *J. comput. Chem.*, **4**, 187.

[38] (a) 'Quanta/CHARMm' (Chemistry at HARvard Macromolecular mechanics). (b) 1990, Quanta Parameters: Release 3.0, Polygon Corporation.

[39] GRIGORAS, S., and LANE, T. H., 1988, *J. comput. Chem.*, **9**, 25.

[40] A common technique applied in the derivation of atomic charges from wave functions rooted in the LCAO (Linear Combination of Atomic Orbitals) approximation is the Mulliken population analysis [MULLIKEN, R. S., 1955, *J. chem. Phy.*, **23**, 1833] used in this study. Note that alternatively, the charges may be extracted by fitting the molecular electrostatic potential [BESLER, B. H., MERZ, K. M. JR., and KOLLMAN, P. R., 1990, *J. comput. Chem.*, **11**, 431]. In Mulliken's scheme it is assumed that the overlap population associated with any atoms *M* and *N* due to AOs of type *k* and *l*, respectively, arising from an *ith* MO (molecular orbital), can be divided equally between the two atoms, and equals $2\,v_i c_{kMi} c_{lNi} S_{kMlN}$ where *c* are the AO coefficients and *S* their overlap integral, and v_i is the occupation number of the *i*th MO. Mulliken's population analysis yields the population on an atom from the appropriate sums over all doubly occupied MOs and over all types of basis functions. Although this scheme has been questioned [MOMANY, F. A., 1982, *J. phys. Chem.*, **82**, 592. WILLIAMS, D. E., and YAN, J. M., 1988, *Adv. atom. molec. Phys.*, **23**, 87], it provides in this case atomic charges which are consistent with those derived by other methods [RAO, P. S., MCEACHERN, R. J., and WEIL, J. A., 1991, *J. comput. Chem.*, **12**, 254. ABRAHAM, R. J., GRANT, G. H., HAWORTH, I. S., and SMITH, P. E., 1991, *J. comput.-aided Molec. Design*, **52**, 21] and justified to be used. The MNDO [DEWAR, M. J. S., and THIEL, W., 1977, *J. Am. chem. Soc.*, **99**, 4899, 4907] (modified neglect of differential overlap) semiempirical technique which invokes the NDO approximation was used [STEWART, J. J. P., 1988, 'MOPAC' version 5.0, *Quant. Chem. Prog. Exch.*, **455**]. The semiempirical

calculation gave a reasonable geometry with the optimized Si–O–Si and O–Si–O ring angles assuming values of 133° and 110°, respectively. A comparison of the MNDO derived partial atomic charges and standard values used by the molecular mechanics force field (in parentheses) for these isomers reveals some differences: O = 0·98 (−0·44); Si = 1·70 (0·53; C = 0·4 to −0·5 (0·02); H(–Si) = 0·03 (−0·02); H(–C) = 0·02 to −0·02 (−0·03). The q(MNDO) values thus derived are consistent with *ab initio* results, and were used for the geometry optimization of the ring system. Optimized structures by CHARMm using either q(MNDO) or q(standard) for the electrostatic contribution to the force field differ by 0·1–0·5 Å RMSD.

[41] PACHTER, R., and WESSELS, P. L., 1988, *J. molec. Struct.* (*Theochem.*), **164,** 189.
[42] PACHTER, R., and WESSELS, P. L., 1988, *J. molec. Struct.* (*Theochem.*), **178,** 323.
[43] MCCAMMON, J. A., and HARVEY, S. C., 1987, *Dynamics of Proteins and Nucleic Acids* (Cambridge University Press).
[44] VAINSTHEIN, B. K., 1966, *Diffraction of X-Rays by Chain Molecules* (Elsevier).
[45] 1990, 'CERIUS' program and manual: release 2.1, Cambridge Molecular Design Corporation.
[46] ALMENNINGEN, A., BASTIANSEN, O., FERNHOLT, L., CYVIN, B. N., CYVIN, S., and SAMDAL, S., 1985, *J. molec. Struct.*, **128,** 59.
[47] CLEBRE, G., DE LUCA, G., LONGERI, M., CATALANO, D., VERACINI, C. A., and EMSLEY, J. W., 1991, *J. chem. Soc. Faraday Trans.*, **87,** 2623.
[48] GRAY, G. W., 1987, *Thermotropic Liquid Crystals* (Wiley).
[49] DAVIDSON, P., and LEVELUT, A. M., 1992, *Liq. Crystals*, **11,** 469.